A 96-well microplate incorporating a replica molded microfluidic network integrated with photonic crystal biosensors for high throughput kinetic biomolecular interaction analysis†

Charles J. Choi and Brian T. Cunningham*

Received 20th December 2006, Accepted 8th March 2007
First published as an Advance Article on the web
DOI: 10.1039/b618584c

A nanoreplica molding process has been used to produce polymer microfluidic channels, with integrated label-free photonic crystal biosensors as the bottom surface of the channels. Multiple flow channels are gathered in parallel so that an imaging detection instrument may simultaneously monitor the binding kinetics of many biomolecular interactions. In this work, the flow channel pattern has been adapted to a 96-well microplate format in which, for each 12-element row of the microplate, a single well serves as a common access port for 11 flow channels that are connected to separate microplate wells. Application of pneumatic pressure or suction to the common well serves to drive forward or backward flow to the channels. The system is demonstrated by measuring the kinetic binding interaction of protein A with IgG molecules of high, medium, and low affinity. The approach offers a means for minimizing the volume of reagent required to functionalize the biosensor surface, while retaining compatibility with the microplate assay fluid-handling methods that are most commonly used in biological research.

Introduction

Label-free sensors typically involve the use of an acoustic, optical, or electrical transducer to indicate the presence of adsorbed biological material on the transducer surface through its mass, dielectric permittivity, conductivity, or capacitance.[1–10] Most often, sensors are integrated with microfluidic channels by fabricating the sensor structure and flow channel structure upon separate substrates, and subsequently aligning the two for bonding with hermetic sealing or an adhesive.[11–13] Transduction is simplified for optical label-free biosensors, such as surface plasmon resonance (SPR) and photonic crystal (PC) devices, that require illumination of the sensor through the substrate and detection of shifts in a resonant coupling condition by measuring the reflected spectrum. For SPR, the highest detection resolution is obtained with the Kretschmann configuration, in which the sensor surface is illuminated through a coupling prism at a single wavelength, over a range of incident angles that incorporates the resonant coupling angle. Systems have been demonstrated that incorporate simultaneous detection of biochemical binding at sampling rates of <1 Hz, from 4–10 flow channels on the same sensor surface.[14,15] Likewise, imaging SPR has been used to monitor kinetic binding information from ~ 100 immobilized protein spots on a sensor surface, exposed to the same analyte in a high resolution endpoint mode,[2] or in a low detection resolution kinetic mode.[16] In each of these cases, the detection regions are small, so that an off-chip fluid handling system and separate chip processing steps are required to prepare the surface chemistry, to add the immobilized ligand, and to introduce the analyte to the proper flow channel—typically by withdrawing fluid from an off-chip multi-well microplate. The tubing, fluid control devices, and optical contact of the sensor to the coupling prism, all represent barriers for adoption by life-science researchers in terms of analyte volume usage, complexity, and cost.

PC biosensors represent a new class of label-free optical biosensors that are capable of detecting biomolecules and cells with high resolution.[6,17] The sensor structure consists of a low refractive index dielectric, patterned with a 1-D sub-wavelength periodic surface grating structure, coated with a thin layer of high refractive index dielectric material. When the sensor surface is illuminated with white light at normal incidence, it reflects only a very narrow resonant band of wavelengths. The resonantly reflected wavelength, called the peak wavelength value (PWV), is modified by the attachment of biomolecules to the sensor surface, so that small changes in surface dielectric permittivity can be quantified with <1 pg mm^{-2} detection resolution without the use of a label.[6] An important property of the PC sensor is that it does not allow lateral propagation of resonantly coupled light. Therefore, a single PC surface is capable of supporting a large number of independent biosensor measurements without optical crosstalk between adjacent sensor regions, enabling high spatial resolution measurement scanning across the sensor surface. Using an image-based sensor scanning method, detection of microarray spots, individual cells, and self-referenced assays within microplates with biosensor pixel resolution as low as 9×9 μm^2 have been performed.[18] Plastic-based PC biosensors have been fabricated over large surface

Nano Sensors Group, Department of Electrical and Computer Engineering, University of Illinois at Urbana–Champaign Micro and Nanotechnology Laboratory 208 N. Wright St. Urbana, IL 61801, USA. E-mail: bcunning@uiuc.edu

† The HTML version of this article has been enhanced with additional colour images.

areas using a roll-to-roll nanoreplica molding process, and incorporated into standard format 96-, 384-, and 1536-well microplates for applications in drug discovery research and molecular diagnostic tests.[6] The PC detection instrumentation does not require a coupling prism for illumination of the sensor, or any other physical contact, so large sensor areas may be scanned rapidly. However, with the ordinary microplate format the reaction kinetics of assays within the plate wells are dominated by the rate of diffusion of analytes to the sensor surface, unless external mixing is provided. Therefore, kinetic biosensor data does not provide reaction rate data on analyte-ligand interactions with the same utility as biosensors incorporated within microfluidic channels, where the analyte diffusion distance is significantly reduced. Further, the microplate format requires tens to hundreds of microlitres of analyte and immobilized ligand solution to coat the active biosensor region in the bottom of the microplate wells. Therefore, it is important to implement PC biosensors in a microfluidic environment to provide the kinetic binding information that is currently available with SPR, but in a format that will increase assay throughput and fluid-handling convenience while reducing cost, reagent volume, and system complexity.

In recent work, we have demonstrated a single-step replica molding process for integrating the fabrication of PC biosensors and microfluidic channels.[19] The process enabled the submicron structure of the PC to be replicated simultaneously with the >10 μm features for the fluid channels, where the sensors were self-aligned with the channels. The process is performed using a room-temperature replica molding process that is performed on flexible plastic substrates for low cost manufacturing. The fabricated sensors within microfluidic channels were measured with a high resolution imaging detection instrument capable of gathering data from multiple points within many flow channels on a single chip.

In this work, we demonstrate a 96-well microplate incorporating a replica molded microfluidic network integrated with PC biosensors. A schematic of the device is shown in Fig. 1. As in our previous work, the microfluidic flow channels and the PC biosensor are co-fabricated and self aligned on a single sheet of flexible plastic. A planar plastic cover is applied over the flow channels to form their upper surface, and to provide holes for fluid access. The microfluidic network assembly is attached with adhesive to a bottomless 96-well microplate, where it forms the bottom surface. The ~1.6 mm diameter holes are arranged so that each microplate well may access the microfluidic network through one hole. As shown in Fig. 1, for a single 12-well row within the microplate, the fluid channels from 11 "analyte" wells are gathered to a single detection region, where all 11 channels may be monitored at once. A central "common" well in each row serves as an access point for introduction of reagents that are identical for all of the flow channels. The common well also serves as a means for applying pressure or suction that will drive fluid from the common well into the flow channels, or to pull fluid from the 11 analyte wells at the same rate. Pneumatic fluid driving force is applied by insertion of a rubber stopper into the common well, with a through-hole connected to a syringe pump. Serpentine flow channel patterns are used to ensure an equal length flow path from each analyte well to the common well. As a result, 88 parallel flow channels integrated with the biosensors with 8 common inlet/outlets are incorporated on the bottom of a 96-well microplate. The microfluidic network configuration incorporated in a microplate-based platform presented in this work enables kinetic binding response measurement across the widths of 11 parallel flow channels in a small area with a high resolution spatial scanning instrument. Therefore, the imaging capability of the scanning instrument may be utilized in two different modes: kinetic mode and imaging mode. The fluid control scheme for this device requires no on-chip active components.

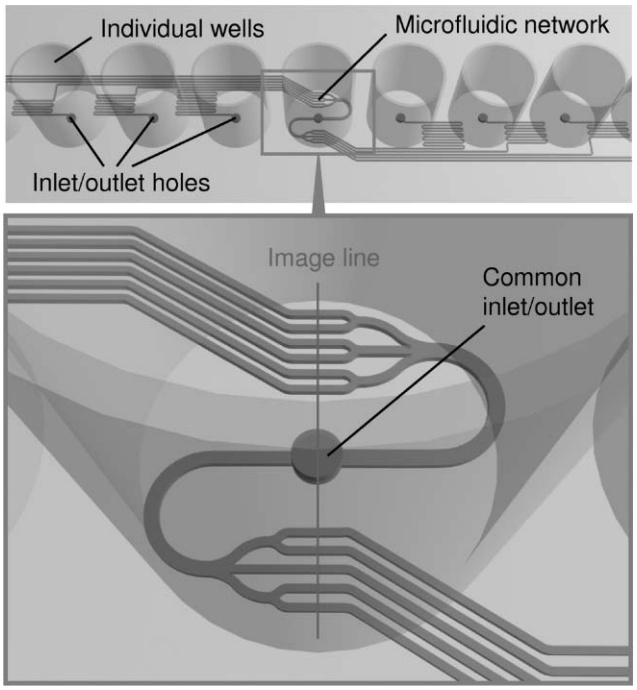

Fig. 1 Schematic of a 96-well microplate incorporating microfluidic network integrated with PC biosensors as bottom surface. A central "common" well in each row serves as an access point for introduction or withdrawal of reagents for the flow channels. Pressure or suction applied at the common well drives fluid from the common well into the flow channels, or pulls fluid from the 11 analyte wells at the same rate. Serpentine flow channel patterns are used to ensure an equal length flow path from each analyte well to the common well. Fluid channels from 11 analyte wells are gathered to a single detection region where all 11 channels may be monitored at once.

Materials and methods

Microfluidic well plate integrated with PC sensor

The fabrication process requires a method that can accurately produce sub-micron features for the PC structure, while at the same time generate >10 μm features for the microfluidic channels. As in previous work, a room-temperature, low-force replica molding method, with a patterned silicon master and a UV curable polymer was used.[19]

First, a silicon wafer was patterned with a 550 nm period 1-D linear grating structure using deep-UV lithography, in which an 8 × 12 array of 6.7 mm diameter circular die,

containing the gratings, were stepped and repeated every 9 mm in the x,y directions. After photoresist development, the patterned grating structure was transferred to the silicon wafer by reactive ion etching, to a depth of 170 nm. Following removal of the photoresist, the fluid channels were patterned onto the same silicon wafer with photoresist using conventional contact lithography. Because high resolution is not required for defining the fluid channels (minimum channel width of 150 μm was used), and to maximize the flexibility for investigating different channel geometries, the photomask for the channel patterns was produced on a transparent plastic film with 5080 dpi resolution printing. After the development of exposed photoresist, fluid channel structures were transferred to the silicon wafer by deep reactive ion etching, to a depth of 20 μm, followed by the removal of photoresist. As a result of the above processing steps, a negative pattern template of microfluidic channels incorporating a sub-micron linear grating was fabricated. The completed silicon master was subsequently treated with dimethyl dichlorosilane (GE Healthcare) to promote clean release of the replica from the master.

Next, the master wafer pattern was replicated onto a 250 μm thick flexible polyethylene terephthalate (PET) substrate. A layer of liquid UV curable polymer was distributed between the silicon wafer and the PET substrate, where the liquid polymer conforms to the shape of the features on the wafer. The liquid polymer was then cured to a solid state by exposure to UV light, and was subsequently released from the wafer by peeling away the PET layer, resulting in a polymer replica of the silicon wafer structure adhered to the PET sheet. The sensor structure was completed by depositing 130 nm of titanium dioxide (TiO_2) on the replica surface using electron beam evaporation. The scanning electron micrographs in Fig. 2 show the cured replica surface coated with TiO_2, in which the replicated flow channel network contains the PC biosensor on the bottom surface.

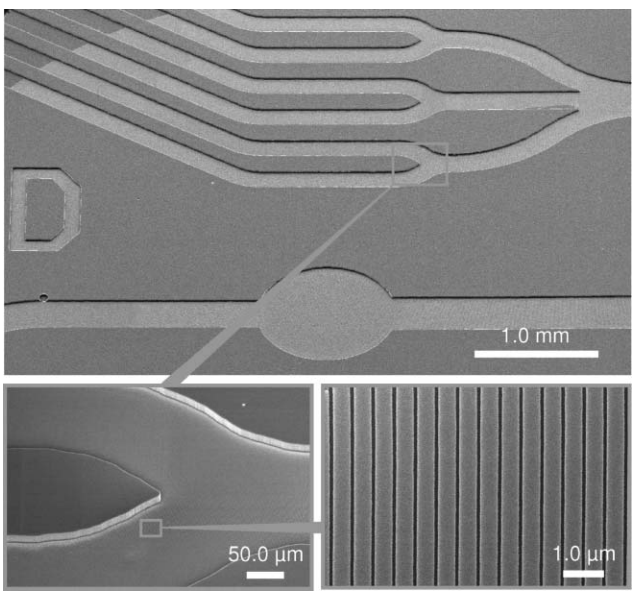

Fig. 2 Scanning electron micrographs of an open microfluidic channel network embedded with the PC biosensor. Cured polymer replica surface is coated with ~130 nm of TiO_2.

The open microfluidic channels were sealed by a separate PET sheet with die-punched 1.6 mm diameter inlet/outlet holes in an 8 × 12 pattern, corresponding to the locations of the wells of a 96-well microplate, using a layer of double sided pressure sensitive adhesive film (3 M). The completed polymer microfluidic network assembly was then attached to a bottomless 96-well microplate (Greiner Bio-One) using an adhesive, as shown in Fig. 3.

Flowing fluids into the microfluidic channels was accomplished by pre-filling one or more inlet holes within the wells of the microplate with solutions, and using pneumatic pressure. With the dimensions of the microfluidic channels used for this device, a minimum of about 20 nL of reagent volume per channel was required to fill the imaging region of the fluid network. After the inlet hole was pre-filled with solution, a rubber cap attached with Teflon micro tubing (Cole–Parmer) was inserted into the opening of the well and a syringe pump (Harvard Apparatus) was used as the pneumatic source to drive the solutions through the microfluidic channels.

Detection instrument

A schematic of the biosensor imaging instrument is shown in Fig. 4. White light illuminates the sensor at normal incidence through a polarization filter, to illuminate with light polarized perpendicular to the sensor grating lines. The reflected light is directed through a beam splitter and an imaging lens to a narrow slit aperture at the input of an imaging spectrometer. Using this method, reflected light is collected from a line on the sensor surface, where the width of the imaged line is determined by the width of the entrance slit of the spectrometer. The imaging spectrometer contains a 2-D CCD camera (Acton Research) with 2048 × 512 pixels. The line of the reflected light containing the biosensor resonance signal is diffracted by a diffraction grating to produce a spatially resolved spectrum from each point within the imaged line. The wavelength of maximum resonant reflection is referred to as the peak wavelength value (PWV), and adsorption of biomolecules results in localized increase in the PWV. When the CCD camera is operated in 2048 × 512 pixel mode, the

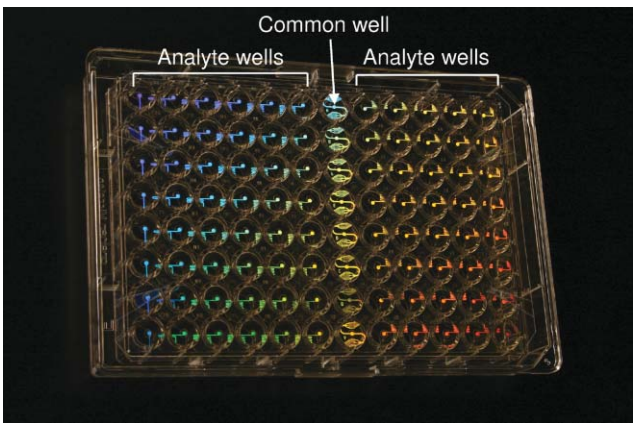

Fig. 3 Photograph of the bottom of the 96-well microplate attached with polymer microfluidic network integrated with PC biosensors.

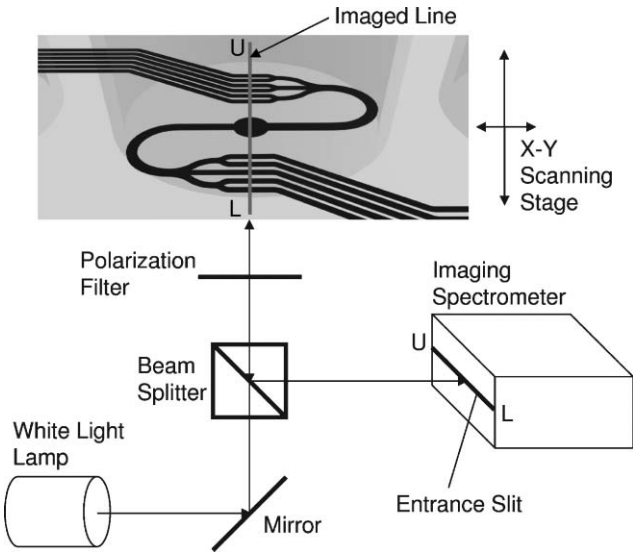

Fig. 4 Schematic of the biosensor imaging instrument. The detection instrument is capable of operating in two different modes: kinetic mode and imaging mode. For the kinetic mode, a motorized stage positions the sensor so that the image line remains fixed upon a single location, so that the image line intersects 11 flow channels and the common port, and the PWV of the PC can be measured continuously as a function of time. For the imaging mode, the motorized stage translates the sensor in a direction perpendicular to the image line in small increments, constructing a spatial map of the PC PWV.

line image through the slit is divided into 512 pixels and a spectrum with a resolution of 2048 wavelength data points is acquired for each of the 512 pixels imaged. Upon peak-finding analysis of all 512 spectra, the PWV for each of the 512 pixels is determined, and thus a line of 512 pixels is generated for the PWV image of the sensor.

Based on the PWV imaging mechanism described above, the detection instrument is capable of operating in two different modes: kinetic mode and imaging mode. For the kinetic mode (measuring ΔPWV as a function of time), a motorized stage positions the sensor so that the image line remains fixed upon a single location that intersects 11 flow channels and the common port, while the PWV of the PC is measured continuously as a function of time. The measurement interval can be designated by software, where the lower limit is determined by the integration time of the CCD chip, data analysis/routing time, and processing load on the computer. For the imaging mode (generating 2-D spatial PWV image of the sensor) however, the motorized stage translates the sensor in a direction perpendicular to the image line in small increments, constructing a spatial map of the PC PWV. The spatial separation of the image lines is determined by the step size of the stage between each image line acquisition. By this technique a series of lines are assembled into an image through a software program, and the same spot in the sensor can be scanned repeatedly after the sensor has been translated. In the current system, the length of the image line is 9.1 mm, as determined by the size of the CCD chip. A large area can be scanned in a serpentine tiled fashion, where the width of a tile is 9.1 mm along the image line direction. For spatial PWV imaging mode, a biosensor experiment typically involves measuring shifts in PWV so the sensor surface is scanned twice; once before and once after biomolecular binding. The images are aligned and subtracted to determine the difference in PWV, as detected by the sensor, and therefore the PWV of the imaged surface is not required to be completely uniform. The PWV pixel resolution, or the width of the imaged line for this work, was 22.3 μm.

Assay reagents

Buffer solution used for the protein–protein interaction assay in this work was phosphate buffered saline (PBS) purchased from Sigma–Aldrich. Protein A (Pierce Biotechnology), prepared in PBS buffer solution at a concentration of 0.5 mg mL^{-1}, was used as the immobilized protein ligand on the sensor surface within the microfluidic channels. The blocking buffer used to prevent nonspecific binding sites for the experiment was Sea Block (Pierce Biotechnology), diluted in PBS with a volume ratio of 1 : 4. The analytes used for the assay were human, pig, rabbit, sheep, goat, rat, and chicken immunoglobulin G (IgG) purchased from Sigma–Aldrich. The IgGs were also prepared in PBS buffer solution at a concentration of 0.5 mg mL^{-1}.

Results

Protein–protein binding assay

An assay characterizing binding affinities of IgGs from various species to protein A was performed to demonstrate the operation and biomolecular detection capability of the microfluidic well plate device.

Protein A was immobilized on the image line region of the sensor surface for one row of the microplate with simple physical adsorption by flowing protein A solution through the common inlet and allowing the solution to incubate at room temperature for 30 min at an average flow rate of $\sim$0.4 μL min^{-1} per channel, followed by a PBS rinse to wash away unbound excess protein molecules. For this experiment, the common inlet was pre-filled with 30 μL of protein A solution (0.5 mg mL^{-1}), though only 220 nL was needed to fill 11 flow channels up to the image line. After protein A adsorption, blocking buffer solution was introduced through the common inlet to the flow channels where it was allowed to incubate at room temperature for 15 min, followed by a PBS rinse. After blocking, a PWV measurement was made in the imaging mode to obtain a 2-D spatial PWV image of the sensor before the introduction of the analytes. Next, inlet holes corresponding to wells 1–6 and 8 were pre-filled with 20 μL of human, pig, rabbit, sheep, goat, rat, and chicken IgG solutions (0.5 mg mL^{-1}), respectively, and wells 9–12 were pre-filled with PBS to be used as negative controls for the experiment (well 7 has the common inlet/outlet hole). After loading the wells with the analyte and buffer solutions, data acquisition from the detection instrument was initiated in kinetic mode, and solutions were pumped through the channels. The kinetic PWV response of the protein A immobilized sensors for exposure to different types of IgG are shown in Fig. 5(a). Because the width of each fluid channel in the data acquisition area was 150 μm, and the pixel resolution for the image line

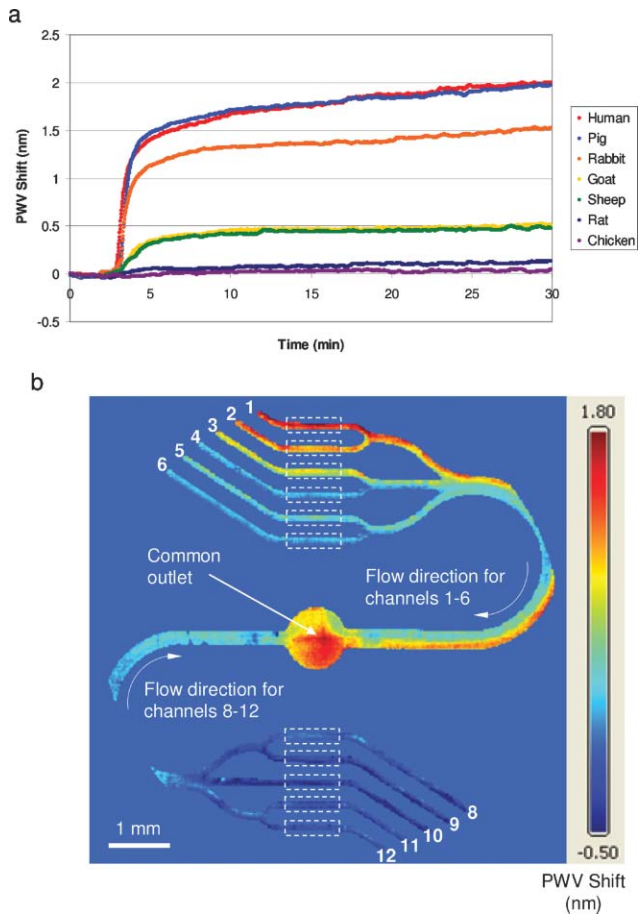

Fig. 5 (a) Kinetic PWV response of the protein A immobilized sensors for different IgG exposure. PWV shifts were obtained by subtracting the average PWVs of the reference channels filled with PBS buffer from the average PWVs obtained for each active channel with IgG. The duration of kinetic measurement was 30 min, with PWV measurements taken at 1.15 s intervals. (b) Spatial PWV shift image obtained from running the detection instrument in imaging mode. PWV shift values were acquired by subtraction of the PWV before analyte introduction from the PWV after analyte introduction on a pixel-by-pixel basis. PWV shifts are represented by the scale bar from −0.50 to 1.8 nm with red regions representing areas of greatest positive shift.

was 22.3 μm, the PWV responses for each channel were calculated by averaging the PWV of each of the 6 pixels within each flow channel. PWV shifts plotted in Fig. 5(a) were obtained by subtracting the average PWVs of the reference channels filled with PBS buffer from the average PWVs obtained for each active channel with IgG. The duration of kinetic measurement was 30 min, with PWV measurements taken at 1.15 s intervals. The length of a flow channel from the analyte well to the common well was 64 mm, with serpentine flow paths of longer lengths incorporated to the flow channels for analyte wells that were closer to the common well. Because pneumatic pressure from the common well was used to drive the flow of liquids to/from all the analyte wells in parallel, flow paths of equal length were required to maintain equal flow rate along all the fluid channels. For the experiment in this work, a syringe pump drew air from the plugged common well at an average rate of 76.5 μL min^{-1}, resulting in an average liquid flow rate of 0.442 μL min^{-1} through the flow channels. The flow rates were separately measured and verified using colored dye solutions, and approximately equal flow rates were observed from each of the analyte wells to the common well, with a maximum difference of 7 s latency between the fastest and slowest channel. Due to the length of the microchannels (serpentine channel patterns were employed to ensure equal channel length for all analyte wells), any minor differences between the fluid flow channels created during the replication/fabrication process of the device could cause differences in flow rates. However, the effect of minor differences of fluid flow rate on kinetic binding results would be negligible since the rate of analyte diffusion to the bottom sensor surface was proportional to the cube root of the fluid flow rate.[20] In addition, biomolecular interaction detection assays should be done under a condition where the interaction between the surface immobilized molecule and the analyte is limited by the reaction rate, rather than the analyte mass transport (diffusion) rate to the sensor surface. Under such a condition, minor differences in analyte mass transport rate do not affect the kinetic results.

After the kinetic PWV measurement, all fluid channels were rinsed with PBS buffer by introducing the buffer solution through each of the analyte channels. Subsequently, an imaging mode measurement was made again to obtain a 2-D spatial PWV shift image of the sensor after the IgG binding. The PWV shift during the assay was obtained by subtraction of the PWV before analyte introduction from the PWV after analyte introduction on a pixel-by-pixel basis, to form the PWV shift image shown in Fig. 5(b), where the PWV shifts are represented by the scale bar from −0.50 to 1.80 nm, with red regions representing areas of greatest positive shift. After the spatial PWV shift image was obtained, a 9 × 41 pixel rectangular region was selected for each flow channel (shown as dashed rectangular areas in Fig. 5(b)), where 369 independent pixel readings within each channel can be averaged into a single endpoint measurement. The average PWV shift for each flow channel containing different analytes for this experiment is shown in Table 1. The flow channels containing only PBS buffer as the analyte were designated as reference channels, and PWV shift for the active channels which were exposed to IgG are reported in Table 1, relative to

Table 1 Average PWV shift for each flow channel containing different analytes, and the active channels (exposed to IgG) with reference channels (exposed to PBS) taken into account. PWV shift values were obtained from averaging 369 independent pixel readings within the rectangular grid selected for each flow channel (shown as dashed rectangular areas in Fig. 5(b)).

Channel	IgG	Avg PWV shift/nm	Avg PWV shift with reference/nm
1	Human	1.497	1.758
2	Pig	1.138	1.399
3	Rabbit	0.775	1.036
4	Sheep	0.185	0.446
5	Goat	0.369	0.630
6	Rat	0.167	0.428
8	Chicken	−0.035	0.226
9–12	PBS buffer	−0.261	—

the average of all 4 reference channels. In the imaging mode, detection of biochemical binding along the bottom surfaces of the channels is obtained, which allows direct visual observation of immobilized ligand density, detected analyte density, and non-uniformities resulting from mass transport limitations along the flow channels. It is interesting to directly observe the preservation of laminar flow in Fig. 5(b), where flow channels 1–6 gather together and combine their streams en route to the common port. As flow channels 1–2 contain the analytes with the highest affinity for protein A, while flow channels 5–6 contain analytes with the lowest affinity, a gradient in PWV shift is observed across the width of the combined flow channel, that is maintained from the flow stream gathering point to the common port.

Discussion

The ability to monitor both kinetic and high resolution endpoint information with a label-free biosensor embedded within a microfluidic channel affords the opportunity to investigate the kinetic on-rates and off-rates of biomolecular binding interactions, under assay conditions that are not limited by analyte diffusion or other mass-transport effects. Furthermore, one can simultaneously observe and verify the uniformity of surface functionalization and analyte detection in both the cross-channel and down-channel directions. Therefore, the imaging capability allows one to determine whether laminar flow conditions exist, and whether analytes (particularly those present at low concentrations) are deposited preferentially on the leading edge of the biosensor active surface.

The microplate–microfluidic channel integrated format described in this work incorporates the traditional advantages of microfluidic channels, such as low fluid volume and reduction of sample evaporation, with an assay format that is readily compatible with liquid pipetting infrastructure that is most commonly available within life science laboratories. The approach of using a single common well to serve as a branching point for multiple analyte wells, where the biosensor data acquisition region is located in close proximity to the common well, allows a short flow path to prepare a group of biosensors with immobilized ligands using an extremely low sample volume, particularly compared to the sample volume required to immobilize a protein on the bottom surface of a microplate. This advantage is particularly important in assays using expensive purified proteins that are not available in large quantities. Although only 0.21 μL of reagent volume was needed for ligand immobilization, a larger volume was used in order to facilitate the experiment. With smaller inlet hole size and smaller well volume (such as used in 384 or 1536-well microplates), the reagent volume required for ligand immobilization or bioassays could be decreased significantly. Because the flow direction for ligand immobilization through the common well is opposite of the flow direction for subsequent analyte detection, the internal surface of the flow path for the analyte molecules can be free from immobilized ligands. Therefore, analyte molecules are less likely to adhere to the flow channel walls, where they cannot contribute to detection.

While the experiment described in this work involved immobilization of a single common ligand for 11 analytes, the microplate–flow channel format may also be reversed, such that the biosensors immobilized with 11 different ligands, which are subsequently exposed to a single common analyte. Such an assay configuration may be preferred in certain situations, for example where the analyte is substantially more expensive than the immobilized ligands.

The integrated biosensor microplate described in this work utilized a single common well to serve as a central hub for 11 analyte wells, in which 11 biosensors were gathered for simultaneous kinetic measurements across the image line of the instrument. Other configurations that afford even greater levels of kinetic assay parallelism may be envisioned. For example, within a 384-well microplate format, a single common well may serve the wells within a 2-well radius, in order to extend the number of analyte wells from 11 to 24, without changing the microfluidic channel widths or spacing presented here. Likewise, the concept may be extended to the increasingly common 1536-well microplate format. In future work, we plan to demonstrate further increases in the assay throughput, and to utilize the system for determining the kinetic binding characteristics/constants of biomolecular interactions.

Conclusion

We have demonstrated a 96-well microplate device incorporating a replica molded microfluidic network integrated with PC biosensors in this work, using a detection instrument that is capable of operating in both kinetic and spatial imaging modes. The device can be inexpensively manufactured and offers a format that is compatible with current pharmaceutical screening laboratory liquid handling methods. Using the sensor and instrument, we demonstrated the detection of multiple antibodies to a common immobilized ligand, in both kinetic and spatial measurement modes.

Acknowledgements

The authors are grateful to Derek Puff at SRU Biosystems for writing the software that enables the kinetic measurements to be performed on the detection instrument. This material is based upon work supported by the National Science Foundation under Award No. DMI 0328162 and 0427657. Any opinions, findings, and conclusions or recommendations expressed in this material are those of the author(s) and do not necessarily reflect the views of the National Science Foundation. The authors also gratefully acknowledge SRU Biosystems for providing financial support for this work, the staff of the Micro and Nanotechnology Laboratory, and the Center for Nanoscale Chemical–Electrical–Mechanical Manufacturing Systems at the University of Illinois at Urbana–Champaign.

References

1 M. A. Cooper, F. N. Dultsev, T. Minson, V. P. Ostanin, C. Abell and D. Klenerman, *Nat. Biotechnol.*, 2001, **19**, 833–837.
2 E. A. Smith and R. M. Corn, *Appl. Spectrosc.*, 2003, **57**, 320A–332A.
3 B. Cunningham, P. Li, B. Lin and J. Pepper, *Sens. Actuators, B*, 2002, **81**, 316–328.

4 B. Cunningham, B. Lin, J. Qiu, P. Li, J. Pepper and B. Hugh, *Sens. Actuators, B*, 2002, **85**, 219–226.
5 B. Cunningham, J. Qiu, P. Li and B. Lin, *Sens. Actuators, B*, 2002, **87**, 365–370.
6 B. T. Cunningham, P. Li, S. Schulz, B. Lin, C. Baird, J. Gerstenmaier, C. Genick, F. Wang, E. Fine and L. Laing, *J. Biomol. Screen.*, 2004, **9**, 481–490.
7 G. F. Zheng, F. Patolsky, Y. Cui, W. U. Wang and C. M. Lieber, *Nat. Biotechnol.*, 2005, **23**, 1294–1301.
8 C. Berggren, B. Bjarnason and G. Johansson, *Electroanalysis*, 2001, **13**, 173–180.
9 M. Hoummady, A. Campitelli and W. Wlodarski, *Smart Mater. Struct.*, 1997, **6**, 647–657.
10 S. Lofas, M. Malmqvist, I. Ronnberg, E. Stenberg, B. Liedberg and I. Lundstrom, *Sens. Actuators, B*, 1991, **5**, 79–84.
11 M. A. Burns, B. N. Johnson, S. N. Brahmasandra, K. Handique, J. R. Webster, M. Krishnan, T. S. Sammarco, P. M. Man, D. Jones, D. Heldsinger, C. H. Mastrangelo and D. T. Burke, *Science*, 1998, **282**, 484–487.
12 E. T. Lagally, C. A. Emrich and R. A. Mathies, *Lab Chip*, 2001, **1**, 102–107.
13 K. S. Ryu, K. Shaikh, E. Goluch and C. Liu, *Appl. Phys. Lett.*, 2006, **88.**
14 T. M. Chinowsky, J. G. Quinn, D. U. Bartholomew, R. Kaiser and J. L. Elkind, *Sens. Actuators, B*, 2003, **91**, 266–274.
15 D. G. Myszka, *Anal. Biochem.*, 2004, **329**, 316–323.
16 J. M. Brockman and S. M. Fernandez, *Am. Lab.*, 2001, **33**, 37–40.
17 B. T. Cunningham and L. Laing, *Exp. Rev. Proteomics*, 2006, **3**, 271–281.
18 B. Lin, P. Li and B. T. Cunningham, *Sens. Actuators, B*, 2006, **114**, 559–564.
19 C. J. Choi and B. T. Cunningham, *Lab Chip*, 2006, **6**, 1373–1380.
20 R. W. Glaser, *Anal. Biochem.*, 1993, **213**, 152–161.

Authors Queries

Journal: **Lab On A Chip**

Paper: **b618584c**

Title: **A 96-well microplate incorporating a replica molded microfluidic network integrated with photonic crystal biosensors for high throughput kinetic biomolecular interaction analysis**

Editor's queries are marked like this... [1], and for your convenience line numbers are indicated like this... 5.

Query Reference	Query	Remarks
1	For your information: You can cite this article before you receive notification of the page numbers by using the following format: (authors), (journal), (year), DOI: 10.1039/(paper number).	
2	Ref. 13: Please provide the following details: page number(s).	